SciEn

Proceedings of 8th International Conference on Mechanical Engineering and Renewable Energy 2025
10-12 December, 2025, Chattogram, BANGLADESH

SciEn Conference Series: Engineering Vol. 4, 2026, pp 642-645 https://doi.org/10.38032/scse.2026.4.297

Optimizing Eco-Friendly Tin Perovskite Solar Cells via Novel Transport Layer configuration using SCAPS-1D Simulation

Muhaiminul Islam, Prasanjit Das, Md Farhan Imtiaz Chowdhury, Wasif Sadman Tanim, Md Fahim Sadat Bari, and Md. Shaib Hossain*

Department of Mechanical Engineering, Chittagong University of Engineering & Technology, Chattogram-4349, Bangladesh

ABSTRACT

This study employs advanced SCAPS-1D simulation to enhance the performance of lead-free $FASnI_3$ perovskite solar cells (PSCs) by integrating non-traditional charge transport materials. A novel device architecture, FTO/ZnO (ETL)/$FASnI_3$/CBTS (HTL)/Au, with limited prior investigation, is systematically optimized by tuning key parameters including absorber thickness, defect density (N_t), acceptor density (N_A), bandgap (Eg), electron affinity (χ), and back-contact work function. Optimization elevates the power conversion efficiency (PCE) from 27.09% to 29.06%, primarily due to an increase in short-circuit current density (Jsc) from 26.54 mA/cm² to 30.68 mA/cm², despite slight reductions in open-circuit voltage (Voc) (1.170 V to 1.129 V) and fill factor (FF) (87.24% to 83.92%). The ZnO/CBTS-based configuration demonstrates superior potential over conventional transport layers. These findings validate $FASnI_3$ as a high-performance, eco-friendly alternative to toxic lead-based perovskites and silicon and highlight ZnO and CBTS as promising low-research-burden materials. This work offers valuable insights for the design of efficient, stable, scalable, and commercially viable lead-free PSCs, contributing to the advancement of sustainable global energy solutions.

Keywords: Perovskite Solar Cells, $FASnI_3$, SCAPS-1D Simulation, Charge Transport Materials, Lead-Free Photovoltaics

1. Introduction

The rapid ascent of perovskite solar cells (PSCs) has marked a transformative era in photovoltaics, with power conversion efficiencies (PCEs) now exceeding 25% [1]. However, the commercial viability and environmental sustainability of this technology are hampered by the presence of toxic lead in the most efficient perovskite compositions [2]. This has spurred intensive research into lead-free alternatives, with tin (Sn) emerging as the most promising successor due to its similar electronic properties [3].

Formamidinium tin iodide ($FASnI_3$) is a particularly attractive lead-free perovskite, offering a suitable bandgap and excellent optoelectronic properties [4]. Despite its potential, the performance of $FASnI_3$-based PSCs still lags behind their lead-based counterparts, partly due to challenges in finding optimal charge transport layers (CTLs) that minimize recombination and facilitate efficient charge extraction [5]. Conventional CTLs like TiO_2 and Spiro-OMeTAD have limitations, including high-temperature processing and instability, respectively.

In this study, we propose a novel device architecture, FTO/ZnO/$FASnI_3$/CBTS/Au, which utilizes zinc oxide (ZnO) as the electron transport layer (ETL) and copper-thiostannate (CBTS) as the hole transport layer (HTL). This specific combination has received limited attention simulation tool to systematically investigate and optimize this structure. Our work focuses on engineering the absorber layer properties and interfaces to unlock the full potential of this eco-friendly PSC configuration, demonstrating a pathway to high efficiency exceeding 29%.

2. Materials and Methods

The numerical simulations were performed using the SCAPS-1D (Solar Cell Capacitance Simulator) software, version 3.3.10, which solves the one-dimensional Poisson's equation and the continuity equations for electrons and holes under steady-state conditions [6]. The simulations were conducted under standard AM 1.5G illumination at a temperature of 300 K.

The proposed device stack is Glass/FTO/ZnO/$FASnI_3$/CBTS/Au. The initial, non-optimized parameters for each layer were adopted from established literature to ensure physical realism [7, 8]. A summary of the key material parameters used for the simulation is provided in Table 1.

The optimization process involved the systematic variation of the following key parameters of the $FASnI_3$ absorber layer:

- Bandgap (E_g): Varied from 1.45 eV to 1.37 eV.
- Electron Affinity (χ): Varied from 4.00 eV to 3.60 eV.
- Acceptor Doping Density (N_A): Varied from 7×10^{16} cm^{-3} to 7×10^{12} cm^{-3}.
- Thickness: Varied from 450 nm to 850 nm.
- Defect Density (N_t): Varied from 10^{15} cm^{-3} to 10^{11} cm^{-3}.
- Back Contact Work Function: Evaluated for various metals (Ag, Cu, W, Au, etc.).

*Corresponding Author Email Address: muhaimin.nubayer37@gmail.com Published By: SciEn Publishing Group

Table 1. Initial Material Parameters for SCAPS-1D Simulation

Electrical Parameter	ZnO	FASnI3	CBTS	FTO
Bandgap (eV)	3.3	1.45	1.9	3.5
Dielectric permittivity (eV)	9	8.2	5.4	9
Thickness (μm)	0.050	0.45	0.100	0.4
CB effective density of states (cm^3)	3.7×10^{18}	1.0×10^{18}	2.2×10^{18}	2.2×10^{18}
VB effective density of states (cm^3)	1.8×10^{19}	1.0×10^{18}	1.8×10^{19}	1.8×10^{19}
Electron affinity (ev)	4	4	3.6	4.3
Electron mobility (cm^2/Vs)	100	2.2×10^{1}	30	2.0×10^{1}
Hole mobility (cm^2/Vs)	25	$2.2 \times 10^{\wedge 1}$	10	1.0×10^{1}
Uniform donor density N_D (cm^3)	1×10^{18}	0	0	1.0×10^{18}
Uniform acceptor density N_A (cm^3)	0	7.0×10^{16}	1×10^{18}	0
Electron thermal velocity (cm/s)	1.0×10^{7}	1.0×10^{7}	1.0×10^{7}	1.0×10^{7}
Hole thermal velocity (cm/s)	1.0×10^{7}	1.0×10^{7}	1.0×10^{7}	1.0×10^{7}
Defect density N_t	1×10^{15}*	1.0×10^{15}	1×10^{15}*	

3. Results and Discussion

3.1. Impact of Absorber Layer Optimization

The initial simulation of the baseline structure yielded a PCE of 27.09% (Jsc = 26.55 mA/cm², Voc = 1.170 V, FF = 87.24%). Systematic optimization led to significant improvements.

Varying the perovskite bandgap revealed a critical trade-off. Reducing the bandgap from 1.45 eV to 1.39 eV enhanced light absorption, increasing Jsc from 26.55 to 29.42 mA/cm². However, this also caused a decrease in Voc due to reduced quasi-Fermi level splitting. The optimal balance was found at Eg = 1.39 eV, maximizing the PCE.

The absorber thickness was optimized based on the quarter-wavelength principle for enhanced light trapping. Increasing the thickness to 650 nm maximized photon absorption, boosting Jsc to 28.09 mA/cm². While thicker layers can increase recombination, the gains in current outweigh the losses for this optimized thickness.

A critical factor was the defect density (N_t). Reducing N_t from 10^{15} cm^{-3} to 10^{14} cm^{-3} significantly suppressed trap-assisted recombination, leading to improvements in all photovoltaic parameters, particularly Voc and FF. The electron affinity was found to be optimal at its highest value of 4.00 eV, as lower values disrupted the favorable conduction band alignment at the ETL/Absorber interface, increasing recombination and severely degrading performance.

3.2. Impact of Back Contact and Final Optimization

The work function of the back contact metal significantly influences the hole extraction efficiency and recombination at the back interface. Metals with high work functions (Φ ≥ 5.1 eV), such as Gold (Au), produced the best performance. Au facilitates the formation of a favorable band bending at the HTL/contact interface, reducing hole accumulation and interface recombination, thereby yielding higher Voc and FF compared to low-work-function metals like Ag.

3.3. Final Optimized Performance and Band Alignment

The culmination of the optimization process—setting E_g=1.39 eV, thickness=650 nm, N_t=1×10^{14} cm^{-3}, N_A=7×10^{14} cm^{-3}, and using an Au back contact—resulted in a dramatically improved device performance. The final optimized parameters are summarized in Table 2, and the corresponding J-V curve is shown in Fig. 1.

Table 2. Device Performance Before and After Optimization

Parameter	Before Optimization	After Optimization
Jsc (mA/cm²)	26.55	30.68
Voc (V)	1.170	1.129
Fill Factor (%)	87.24	83.92
PCE (%)	27.09	29.06

The reduction in Voc and fill factor is likely due to increased charge recombination and higher series resistance introduced during the optimization process. These factors slightly hinder charge extraction despite improved current generation.

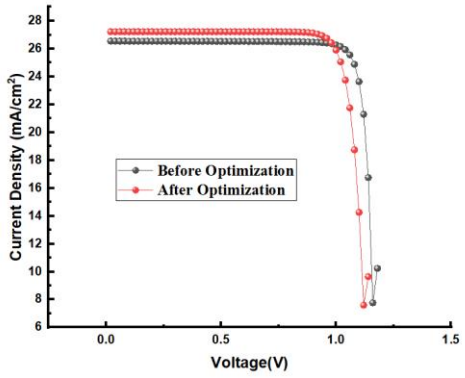

Fig. 1. J-V characteristics of the proposed PSC before and after optimization

The energy band diagram analysis, shown in Fig. 2, provides a physical explanation for the performance enhancement. In the optimized device, the conduction band offset at the ZnO/$FASnI_3$ interface is transformed from a "cliff" to a more favorable "spike," which effectively blocks hole backflow and reduces electron recombination. Similarly, the valence band alignment at the $FASnI_3$/CBTS interface is improved, enhancing hole transport and blocking electrons. These optimized interfaces are crucial for the observed high efficiency.

While Zinc Oxide ZnO is an attractive Electron Transport Layer (ETL) due to its high electron mobility and low-temperature processing, it presents a critical stability issue when in direct contact with organic-cation-based perovskites $FASnI_3$. To successfully use ZnO as an ETL, a buffer layer or chemical modification is required to prevent this direct, destructive contact. The two most common and effective strategies are the use of a SnO_2 buffer layer or doping the ZnO with Aluminum (AZO).

3.3 Discussion on Device Stability and Fabrication Feasibility

This bilayer can be fabricated using common lab techniques, such as Atomic Layer Deposition (ALD) or by spin-coating the different layers sequentially.

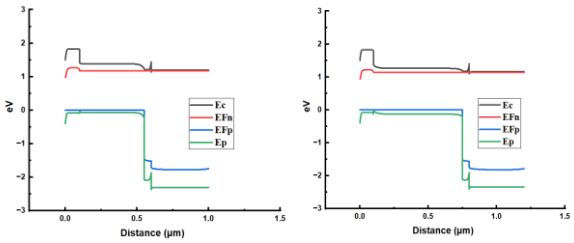

Fig. 2. Energy band alignment of the solar cell (a) before and (b) after optimization.

Table 4.1 Comparative analysis of Previous and presented work.

Solar Cell Structure	Voc (V)	Jsc (mA/cm^2)	FF (%)	PCE (%)	References
ITO/PEDOT: PSS/FASnI3/$PC_{60}BM$ /PEI/Ag	0.64	15.36	56	5.51	[9]
FTO/PC61BM/FASnI 3/PEDOT:PSS+Wo3/ Cu	1.12	24.65	86.02	23.69	[10]
FTO/ZnO/$FASnI_3$/Spi ro- OMeTAD	1.06	16.71	85.85	19.80	[11]
FTO/TiO2/$FASnI_3$/Sp iro-OMeTAD	1.81	31.20	33.72	19.08	[12]
FTO/PCBM/$FAPbI_3$/ CuI	1.14	21.64	70.93	17.61	[13]
FTO/CeO_2/$FASnI_3$/C uI/Au	0.9308	30.675	87.10	24.87	[7]
FTO/$Zn_{0.3}S_{0.7}$/$FASnI_3$ /CuSCN/Au	1.0859	28.12	84.96	25.94	[14]
FTO/C_{60}/$FASnI_3$/$CuS bS_2$/Au	0.74	26.15	83.38	16.05	[15]
FTO/ZnO/$FASnI_3$/CB TS/Au	1.13	30.68	83.92	29.06	This Work

4. Conclusion

This simulation study successfully demonstrates the high potential of a novel, lead-free PSC architecture utilizing ZnO and CBTS as charge transport layers. Through meticulous optimization of the $FASnI_3$ absorber layer and back contact, a champion power conversion efficiency of 29.06% was achieved. The results highlight the critical importance of bandgap tuning, defect minimization, optical thickness management, and proper interface engineering. The ZnO/CBTS pair is validated as a highly effective charge transport configuration for tin-based perovskites. This work provides a clear and promising design blueprint for the experimental fabrication of efficient, stable, and environmentally friendly perovskite solar cells, contributing significantly to the development of sustainable photovoltaic technologies.

5. Acknowledgement

We sincerely express our deepest gratitude to Professor Dr. Prasanjit Das, Department of Mechanical Engineering, CUET, for their invaluable guidance, insightful feedback, and continuous encouragement throughout this work.

6. References

[1] M. Green, et al., "Solar cell efficiency tables (Version 57)," *Progress in Photovoltaics: Research and Applications*, vol. 29, no. 1, pp. 3-15, 2021.

[2] M. Ren, et al., "Potential lead toxicity and leakage issues on lead halide perovskite photovoltaics," *Journal of Hazardous Materials*, vol. 426, p. 127848, 2022.

[3] W. Ke, et al., "'Unleaded' Perovskites: Status Quo and Future Prospects of Tin-Based Perovskite Solar Cells," *Advanced Materials*, vol. 31, no. 47, p. 1803230, 2019.

[4] W. Gao, et al., "Robust Stability of Efficient Lead-Free Formamidinium Tin Iodide Perovskite Solar Cells Realized by Structural Regulation," *The Journal of Physical Chemistry Letters*, vol. 9, no. 24, pp. 6999-7006, 2018.

[5] A. Tara, et al., "Device simulation of FASnI3 based perovskite solar cell with Zn(O0.3, S0.7) as electron transport layer using SCAPS-1D," *Optical Materials*, vol. 119, p. 111362, 2021.

[6] M. Burgelman, et al., "Modelling polycrystalline semiconductor solar cells," *Thin Solid Films*, vol. 361, pp. 527-532, 2000.

[7] A. U. Rehman, et al., "Performance optimization of FASnI3-based perovskite solar cell through SCAPS-1D simulation," *Hybrid Advances*, vol. 7, p. 100301, 2024.

[8] M. K. Hossain, et al., "An extensive study on multiple ETL and HTL layers to design and simulation of high-performance lead-free CsSnCl3-based perovskite solar cells," *Scientific Reports*, vol. 13, no. 1, p. 2521, 2023.

[9] L. Peng and W. Xie, "Theoretical and experimental investigations on the bulk photovoltaic effect in lead-free perovskites $MASnI_3$ and $FASnI_3$," *RSC Adv.*, vol. 10, no. 25, pp. 14679–14688, 2020, doi: 10.1039/D0RA02584D.

[10] H. Alipour and A. Ghadimi, "Optimization of lead-free perovskite solar cells in normal-structure with WO 3 and water-free PEDOT: PSS composite for hole transport layer by SCAPS-1D simulation," *Opt. Mater.*, vol. 120, p. 111432, Oct. 2021, doi: 10.1016/j.optmat.2021.111432.

[11] Y. El Arfaoui, M. Khenfouch, and N. Habiballah, "Optimization of all Pb-free perovskite CsGeI3/FASnI3 tandem solar device with 30.42% efficiency: Numerical simulation using SCAPS," *Optik*, vol. 300, p. 171638, Apr. 2024, doi: 10.1016/j.ijleo.2024.171638.

[12] N. K. Singh, A. Agarwal, A. K. Singh, and S. N. Singh, "Design and performance evaluation of eco-friendly FASnI3/CsSn0.5Ge0.5I3 based perovskite solar cell with distinct charge transport layer: A computational modeling," *Sol. Energy*, vol. 268, p. 112256, Jan. 2024, doi: 10.1016/j.solener.2023.112256.

[13] M. Noman, M. Shahzaib, S. T. Jan, Z. Khan, M. Ismail, and A. D. Khan, "Optimizing band gap, electron affinity, & carrier mobility for improved performance

of formamidinium lead tri-iodide perovskite solar cells," *Mater. Sci. Eng. B*, vol. 300, p. 117114, Feb. 2024, doi: 10.1016/j.mseb.2023.117114.

[14] A. Tara, V. Bharti, S. Sharma, and R. Gupta, "Device simulation of FASnI3 based perovskite solar cell with Zn(O0.3, S0.7) as electron transport layer using SCAPS-1D," *Opt. Mater.*, vol. 119, p. 111362, Sep. 2021, doi: 10.1016/j.optmat.2021.111362.

[15] D. Azhakanantham, M. Selvamani, T. Geun Kim, D. Contreras, and A. Varman Kesavan, "Exploring novel HTL suitable for Eco-friendly and high performance FASnI3 photovoltaics," *Mater. Sci. Eng. B*, vol. 284, p. 115909, Oct. 2022, doi: 10.1016/j.mseb.2022.115909.

7. Nomenclature

Symbol	Meaning	Unit
Roman Symbols		
A,B,X	Cations and anions in the ABX_3 perovskite structure	Dimensionless
E_g	Bandgap energy	(eV)
FF	Fill factor	(%)
G	Carrier generation rate	($cm^{-3}s^{-1}$)
J,Jsc	Current density, Short-circuit current density	(mA/cm^2)
J_n,J_p	Electron and hole current density	(mA/cm^2)
n,p	Electron and hole concentration	(cm^{-3})
N_A,N_D	Acceptor and donor density	(cm^{-3})
N_C,N_V	Effective density of states (Conduction/Valence band)	(cm^{-3})
N_t	Defect density	(cm^{-3})
PCE	Power conversion efficiency	(%)
q	Elementary charge	(C)
T	Temperature	(K)
U	Recombination rate	($cm^{-3}s^{-1}$)
V,V_{oc}	Voltage, Open-circuit voltage	(V)
Greek Symbols		
χ	Electron affinity	(eV)
ε	Dielectric permittivity	Dimensionless
μ_n,μ_p	Electron and hole mobility	($cm^2/V{\cdot}s$)
Φ	Work function	(eV)
Acronyms		
AM1.5G	Air Mass 1.5 Global (solar spectrum)	
CBTS	Copper Thiostannate (HTL material)	
ETL	Electron Transport Layer	
$FASnI_3$	Formamidinium Tin Iodide (absorber)	
FTO	Fluorine-Doped Tin Oxide (electrode)	
HTL	Hole Transport Layer	
PSC	Perovskite Solar Cell	
SCAPS-1D	Solar Cell Capacitance Simulator (software)	
ZnO	Zinc Oxide (ETL material)	